

# Investigation of the influence of high molecular weight polyethylene and basalt content used in three-dimensional weft-knitted fabrics on the mechanical risks

Textile Research Journal

0(0) 1–13

© The Author(s) 2022



Article reuse guidelines:

[sagepub.com/journals-permissions](https://sagepub.com/journals-permissions)

DOI: 10.1177/00405175221109633

[journals.sagepub.com/home/trj](https://journals.sagepub.com/home/trj)

Julija Krauledaitė<sup>1</sup> , Kristina Ancutienė<sup>1</sup>, Sigitas Krauledas<sup>2</sup>,  
Virginijus Urbelis<sup>3</sup> and Virginija Sacevičienė<sup>4,5</sup>

## Abstract

This study investigates the resistance of three-dimensional (3D) weft-knitted fabrics to mechanical risks in order to determine the impact of the percentage content of raw materials in the knits on mechanical loads. For this purpose, 3D weft-knitted fabrics, consisting of a front side, binding, and back side layers, were designed and produced on an E20 circular weft-knitting machine using organic multifilament yarns (high molecular weight polyethylene, HMWPE) and inorganic multifilament (basalt, BS) yarns for the front and back side layers and conventional polyamide yarns for the binding layer. The cut, puncture, abrasion, and tear resistance tests were performed to assess the resistance of 3D weft-knitted fabrics to mechanical risks. According to the testing results, basalt in the structure of 3D weft-knitted fabrics significantly increases the cut resistance, even in cases of a small basalt content in the knit. The puncture, abrasion, and tear resistance testing results showed that the highest HMWPE percentage content in the knitted structure provided the highest resistance to these risks, while increasing the basalt content in the knit did not improve the resistance testing results. Based on the testing results and the assessment of the protection levels provided by the knitted fabrics, the conclusion can be made that the use of HMWPE multifilament yarns and basalt multifilament yarns in the structure of 3D weft-knitted fabrics contributes to the achievement of the highest levels of performance. All the designed 3D weft-knitted fabrics provide complex protection against different mechanical risks (cut, puncture, abrasion, tear). The tests performed may be useful for further development of knitted fabrics designed to provide protection against mechanical risks.

## Keywords

Three-dimensional (3D) weft-knitted fabric, high molecular weight polyethylene (HMWPE), basalt, cut resistance, puncture resistance, abrasion resistance, tear resistance, mechanical risk

Every year, many workplace injuries occur in the world. Cuts and puncture hazards are considered as the most dangerous risks to the health of people working in mechanical areas.<sup>1</sup> According to the US Bureau of Labor Statistics, 2.8 out of every 100 workers were injured at their workplace.<sup>2</sup> Protective clothing is necessary to prevent injuries.<sup>3</sup> Recently, many studies have focused on the abilities of fabrics to protect the human body<sup>4,5</sup> because the need to ensure safety and protection of workers is increasing.<sup>6</sup>

Hands are the most frequently injured part of the body at work.<sup>7</sup> Therefore, the largest demand in the

<sup>1</sup>Department of Production Engineering, Kaunas University of Technology, Lithuania

<sup>2</sup>Center for Physical Sciences and Technology, Lithuania

<sup>3</sup>Department of Product Development, Granberg AS, Norway

<sup>4</sup>Research Laboratory, UAB Granberg LT, Lithuania

<sup>5</sup>Kaunas University of Technology, Lithuania

## Corresponding author:

Julija Krauledaitė, Kaunas University of Technology, Studentų g. 56, Kaunas, 51424 Lithuania.

Email: [julija.krauledaite@ktu.edu](mailto:julija.krauledaite@ktu.edu)

personal protective equipment (PPE) market is hand protection with a share of 25% of the total, and this market continues to grow.<sup>6</sup> Thanks to hand protective clothing, made of high-performance materials, the situation is improving, but there is still room for improvement.<sup>7</sup>

Organic (aramids, extended chain polyethylenes, aromatic polyester fibers, etc.) and inorganic fibers (glass, basalt (BS), carbon, metals, etc.) are used to create high-performance structures.<sup>8–10</sup> The protective clothing is mostly based on high-performance fibers.<sup>11</sup> Special organic fibers, such as carbon, para-aramids, and high molecular weight polyethylene (HMWPE), as well as inorganic fibers, such as glass, are used for this purpose.<sup>12</sup> High-performance fibers can be part of today's and tomorrow's solutions for high-tech products.<sup>13</sup>

Basalt fiber (BF) is known as the new material of the 21st century,<sup>14</sup> and is widely used in the military and civilian fields. Up until now BS fabrics have not been recognized as a material for PPE; rather, they have been used mostly for technical purposes.<sup>15</sup> BF has high potential to replace glass fiber in today's culture of stringent environmental concern,<sup>16</sup> due to the similar properties and lower price compared with aramid, carbon, and UHMWPE fiber.<sup>17–21</sup> It is considered that the mechanical performance of BF is between those of glass and carbon fibers.<sup>20,22,23</sup> BF is characterized by higher values of tensile strength and Young's modulus.<sup>19–21,24–26</sup> BF may be a great alternative to the glass fibers currently used in protective clothing production and can be used in high-performance applications.<sup>6,15,20,21,24,27</sup> Although the application of BF is expanding, research of BF in the protection field is still in the primary stage.<sup>6,18,28</sup>

In recent years, more attention has been paid to BF in the composite industry as it can replace glass or carbon fibers for composite reinforcement.<sup>22,23,25</sup> Compared with glass, carbon, and aramid fiber, BF has good mechanical properties, and therefore can enhance the material properties of the composite.<sup>18–20,29</sup> BF used as a reinforcement can make a variety of composites with excellent performance that are therefore attractive for protective clothes, bullet proof vests, etc.<sup>5,20,30</sup>

For human body protection, various types of composites are used, reinforced with either high-performance fibers or with the usage of a two-dimensional textile structure.<sup>5</sup> Inorganic fibers, such as carbon, glass, and BS, are widely used to create high-performance structures.<sup>10,31</sup> Further research is needed due to the complex mechanism and also diversity in using various fibers and various structures.<sup>31</sup> As for a composite material, performance depends not only on the strength of the constituent materials but

also on the internal structural geometry of the constituents.<sup>32</sup>

Whereas research is mainly focused on carbon fiber and glass fiber composites, more attention should be paid to the mechanical properties of BF and its usage for protective textiles against hazardous risk. Research on BF and its use in textiles designed to provide protection against mechanical risks is still in its early stages. The aim of this study was to design the structure of three-dimensional (3D) weft-knitted fabrics allowing for positioning of technical yarns (HMWPE and BS) in the front and back side layers of the knit and to determine the impact of the varied composition content on the resistance of fabrics to mechanical risks, that is, cut, puncture, abrasion, and tear.

## Materials and methods

### Knitted fabrics

A 3D knitted fabric structure, consisting of separate front side and back side layers that are connected by a separate binding layer, has been chosen for the study. Eight different 3D knitted fabrics were designed and produced on an E20 circular weft-knitting machine. Figure 1 shows the knitting notation of the 3D weft-knitted fabric, while Figure 2 presents the view of the designed knitted fabrics.

Three types of yarns were used to produce 3D weft-knitted fabrics in this study: HMWPE multifilament yarns, BS multifilament yarns, and polyamide (PA) (Table 1). In the front and back side layers, HMWPE multifilament yarns (22.2 × 2 tex, 120 filaments, twisted in the S direction (100 m<sup>-1</sup>)) and/or BS multifilament yarns (22.2 tex) twisted with HMWPE (22.2 tex) (HMWPE + BS) in the S direction

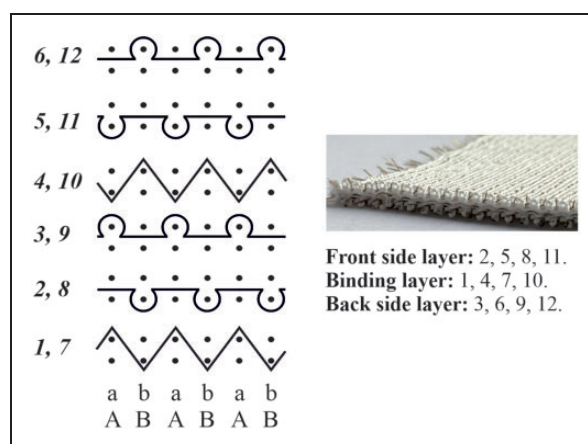


**Figure 1.** The knitting notation (where AB and ab denote the needle set up: AB – the cylinder needles, ab – the disc needles) and sample of the three-dimensional weft-knitted fabric.

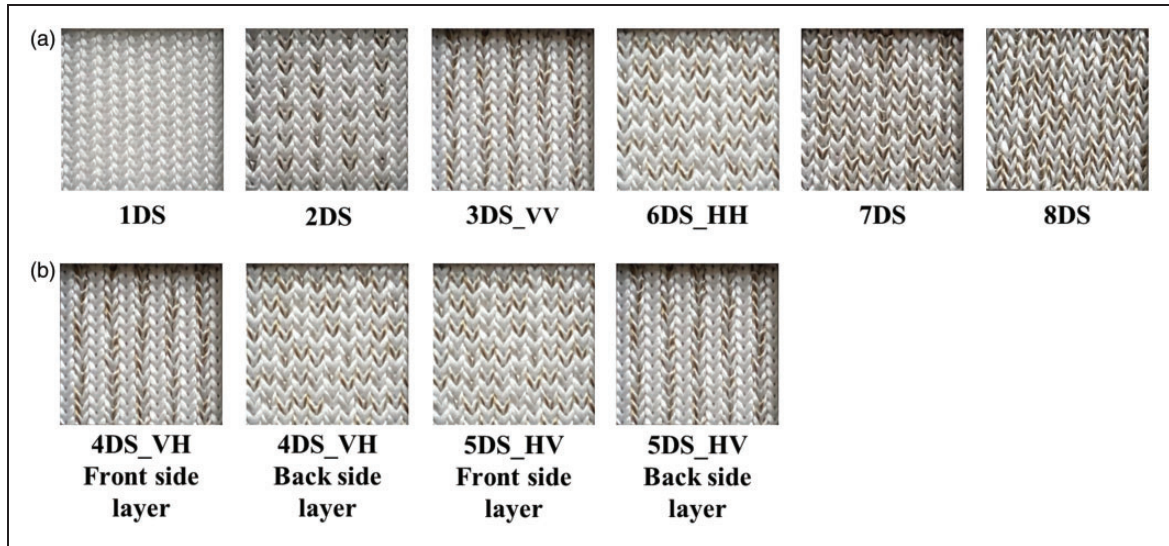


**Figure 2.** The view of the three-dimensional weft-knitted fabrics: (a) the front side and back side layers seem the same and (b) the front side and back side layers are different.

**Table 1.** Arrangement of yarns in the layers

Knitted fabric symbol	Type of yarn	Arrangement of yarns
1DS	HMWPE	2, 5, 8, 11 (front side)
	PA	1, 4, 7, 10 (binding)
2DS	HMWPE	3, 6, 9, 12 (back side)
	HMWPE, HMWPE + BS	2, 5, 8 (HMWPE); 11 (HMWPE + BS) (front side)
3DS_vv	PA	1, 4, 7, 10 (binding)
	HMWPE, HMWPE + BS	3, 6, 9 (HMWPE); 12 (HMWPE + BS) (back side)
	HMWPE, HMWPE + BS	2, 8 (HMWPE); 5, 11 (HMWPE + BS) (front side)
4DS_VH	PA	1, 4, 7, 10 (binding)
	HMWPE, HMWPE + BS	3, 9 (HMWPE); 6, 12 (HMWPE + BS) (back side)
	HMWPE, HMWPE + BS	2, 8 (HMWPE); 5, 11 (HMWPE + BS) (front side)
5DS_HV	PA	1, 4, 7, 10 (binding)
	HMWPE, HMWPE + BS	3, 6 (HMWPE); 9, 12 (HMWPE + BS) (back side)
	HMWPE, HMWPE + BS	2, 5 (HMWPE); 8, 11 (HMWPE + BS) (front side)
6DS_HH	PA	1, 4, 7, 10 (binding)
	HMWPE, HMWPE + BS	3, 9 (HMWPE); 6, 12 (HMWPE + BS) (back side)
	HMWPE, HMWPE + BS	2, 5 (HMWPE); 8, 11 (HMWPE + BS) (front side)
7DS	PA	1, 4, 7, 10 (binding)
	HMWPE, HMWPE + BS	3, 6 (HMWPE); 9, 12 (HMWPE + BS) (back side)
	HMWPE, HMWPE + BS	11 (HMWPE); 2, 5, 8 (HMWPE + BS) (front side)
8DS	PA	1, 4, 7, 10 (binding)
	HMWPE, HMWPE + BS	12 (HMWPE); 3, 6, 9 (HMWPE + BS) (back side)
	HMWPE + BS	2, 5, 8, 11 (front side)
	HMWPE + BS	3, 6, 9, 12 (back side)

HMWPE: high molecular weight polyethylene; PA: polyamide; BS: basalt.

( $100\text{m}^{-1}$ ) were chosen because of their exceptional properties to resist mechanical risks. In the binding layer, synthetic elastic textured PA yarns ( $3.2 \times 2$  tex, 10 filaments) were used to connect the front and back side layers.

The objects of this study can be divided into two groups, as follows.

- (1) Knitted structure with a varied HMWPE and BS percentage content: 1DS, 2DS, 3DS-6DS, 7DS,

8DS (the first symbol (1–8) indicates the number of the knitted fabric, the second symbol (DS, double-sided) indicates that both sides of the knitted fabric are suitable for use for protection against mechanical risks).

- (2) Knitted structure with varied positioning of technical yarns (HMWPE and HMWPE + BS) in the front and back side layers of 3D weft-knitted fabrics. (3DS\_VV, 4DS\_VH, 5DS\_HV, 6DS\_HH; here, the letters (VV, VH, HV, HH) denote the arrangement of HMWPE + BS yarns in the front and back side layers. The first letter denotes the arrangement of HMWPE + BS yarns in the front side layer (V – vertically, H – horizontally) and the second letter denotes the arrangement of HMWPE + BS yarns in the back side layer):
- 3DS\_VV with vertically positioned HMWPE + BS in both front side and back side layers;
  - 4DS\_VH with vertically positioned HMWPE + BS in the front side layer and horizontally positioned HMWPE + BS in the back side layer;
  - 5DS\_HV with horizontally positioned HMWPE + BS in the front side layer and vertically positioned HMWPE + BS in the back side layer;
  - 6DS\_HH with horizontally positioned HMWPE + BS in both the front side and back side layers.

### Testing methods

All the developed knitted fabrics were conditioned for 24 h under standard alternative conditions prior to the experimental procedures (EN ISO 139:2005<sup>33</sup>). The following structural parameters of the 3D weft-knitted fabrics were determined in accordance with the related standards: EN ISO 5084:2000 (thickness)<sup>34</sup> and EN

ISO 12127:1999 (mass per unit area, Figure 3).<sup>35</sup> The thickness of all 3D weft-knitted fabrics was uniform and was  $1.59 \pm 0.02$  mm.

The percentage of raw materials *RM* (Figure 3) for each 3D weft-knitted fabric was defined by using 100 mm × 100 mm size specimens. An equal number of rappings were unraveled from each layer of specimen, that is, the front side, binding, and back side. HMWPE + BS were untwisted by separating HMWPE and BS yarns from each other. All yarns were separated by raw material (HMWPE, PA, BS) and weighed using electronic laboratory textile scales. The percentage of raw materials *RM* was calculated by Equation (1)

$$RM = \frac{m}{M} \cdot 100 \quad (1)$$

where *RM* is the percentage of raw materials (%), *m* (g) is the mass of raw material in each separate layer, and *M* (g) is the total mass of raw material in three layers, that is, the front side, binding, and back side.

The cut resistance testing with a straight blade was performed on three specimens for each knitted fabric in accordance with the EN ISO 13997:1999 standard.<sup>36</sup> For this purpose, a SATRA STM 610 cut resistance evaluator was used. The puncture, abrasion, and tear resistance tests were performed in accordance with the EN 388:2016 standard.<sup>37</sup> A SATRA STM 566 tensile testing machine was used for the puncture resistance testing to determine the force required to cause a standard puncture needle to break through a knitted fabric. The test was performed at a test speed of 100 mm/min on four different specimens for each knitted fabric. A SATRA STM 633 Martindale abrasion machine

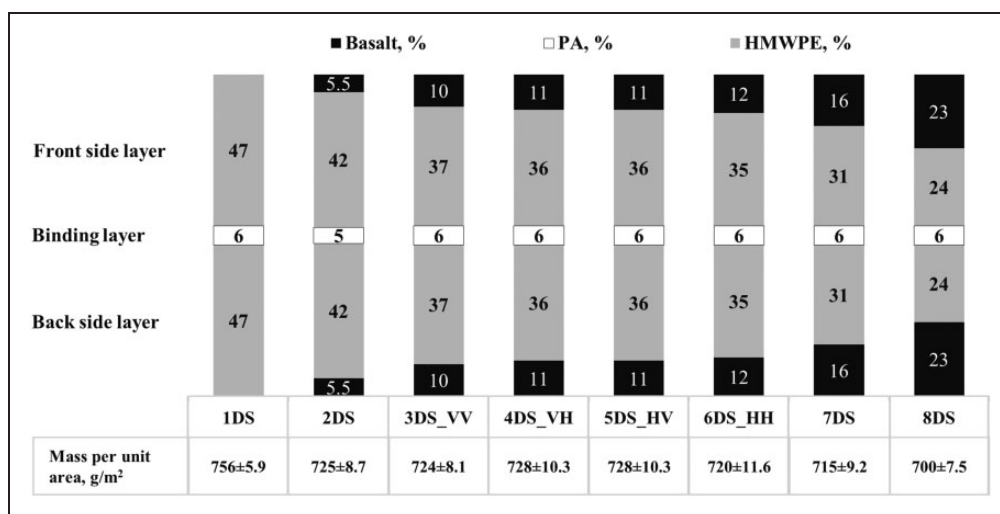


**Figure 3.** The percentage of raw materials *RM* and mass per unit area of three-dimensional weft-knitted fabrics. PA: polyamide; HMWPE: high molecular weight polyethylene.



was used for the abrasion resistance testing to determine the number of rubs required for breakdown to occur, that is, a hole through the specimen to appear. Four different specimens of the knitted fabric were abraded under 9 kPa pressure using an abrasive paper (grit 180, grain type: aluminum oxide). Double-sided adhesive tape was used to provide adhesion of the specimen during the test. The specimens were cleaned in accordance with the EN 388:2016 standard, that is, after 100, 500, 2000, and 8000 cycles. If no breakdown was observed in the fabric after 8000 cycles, the specimens were cleaned every 2000 cycles. A SATRA STM 566 tensile tester was used to determine the maximum force necessary to propagate a tear in a rectangular specimen of the 3D knitted fabric slit halfway along its length. Trouser-type samples (100 mm × 50 mm) with an incision in the longitudinal direction of the sample (25 mm from the edge) were measured, that is, four specimens were cut both in the course direction and the wale direction. The test was performed at a test speed of 100 mm/min. All levels of performance achieved during the straight blade cut, puncture, abrasion, and tear resistance tests were assessed in accordance with the EN 388:2016 standard (Table 2), where Level A/Level 1 represents the lowest and Level F/Level 4 the highest protection level. All the results were supported by basic statistical analysis. The

Duncan test with a significance level of  $\alpha=0.05$  was performed in order to verify and compare the cut, puncture, abrasion, and tear testing results.

## Results and discussion

### Cut resistance

The cut resistance testing results (Figure 4) show that 3D weft-knitted fabric 1DS with the highest HMWPE content in the structure as compared to other tested fabrics required the lowest load to cut.

BS in the knitted structure significantly changed the results obtained, that is, the cut resistance of the knitted fabric 2DS with the 11% BS and 84% HMWPE content (Figure 3) increased 3.98-fold as compared to the 1DS produced with no BS. This significant change can be explained by the presence of BS yarns, which have a very high cut resistance. Various researchers have analyzed the behavior of textiles in terms of the cut resistance and found that specimens containing inorganic fibers (fiberglass or BS) demonstrated the best cut resistance.<sup>38,39</sup> Thus, inorganic fibers can significantly improve the cut resistance of textiles. The cut resistance of fiberglass and BS can be explained by their relative hardness and expected higher transverse mechanical properties.<sup>31</sup>

**Table 2.** EN 388:2016 performance levels<sup>37</sup>

Test	Level A	Level B	Level C	Level D	Level E	Level F
TDM: cut resistance (N)	2	5	10	15	22	30
Test	Level 1	Level 2	Level 3		Level 4	
Puncture resistance (N)	20	60	100		150	
Abrasion resistance (number of cycles)	100	500	2000		8000	
Tear resistance (N)	10	25	50		75	

TDM: Tomodynamometer.

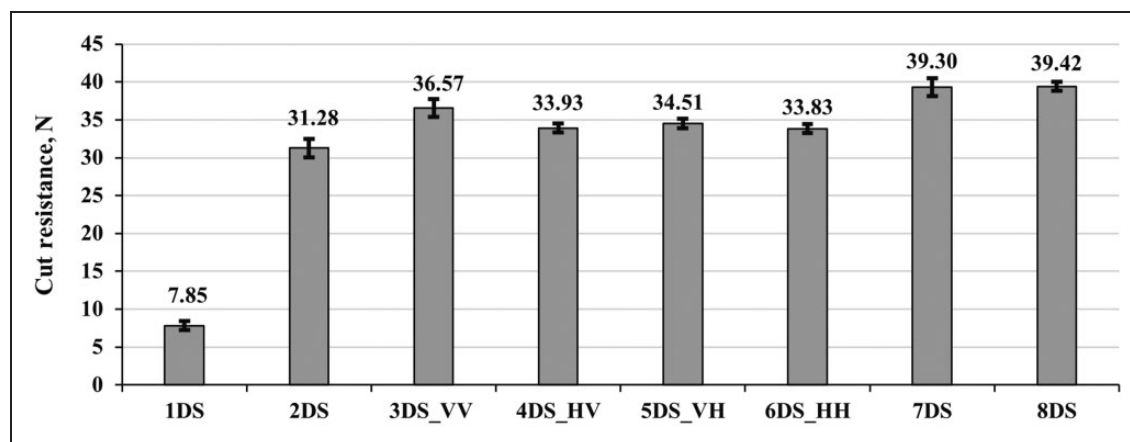


**Figure 4.** Cut resistance testing results.

Analysis of the relationship between the cut resistance (Figure 4) and the percentage content of raw materials (Figure 3) revealed that even a minimal BS content significantly improved the cut resistance, as a higher load was required to cut the BS-containing knitted fabric. The minimal BS content (11%) in the structure significantly increased the cut resistance – even 3.98-fold as compared to the 1DS. Subsequent increases in the BS content did not result in any significant changes, as the cut resistance varied by ~8%. Thus, the optimal cost-effective BS content in the 3D weft-knitted fabric is 20% (3DS\_VV), as further increase of this value does not change the cut resistance significantly.

Results obtained in the 3D weft-knitted fabric group with varied positioning of technical yarns (HMWPE, HMWPE + BS) in the front and back side layers suggest that the cut resistance can be improved, although minimally, by changing the positioning of BS in the structure. Testing of the knitted fabrics with a varied structure and similar composition (3DS-6DS) revealed a higher cut resistance of the 3DS\_VV as compared to the other fabrics tested, which indicates the importance of technical yarn positioning in the protective knitted fabrics, as it can improve the cut resistance without changing the percentage content of raw materials. The optimal BS content and proper yarn positioning in the structure of the 3D fabric give the combined result of high cut resistance.

The results of the studies of cut resistance have been evaluated statistically using the Duncan test (Table 3). It was confirmed that there exists a significant difference between 8DS, 3DS\_VV, 6DS\_HH, 2DS, and 1DS knitted fabrics at the 5% significance level. Thus, not only the changed amount of HMWPE and BS in the structure of the 3D weft-knitted fabric, but also the arrangement of HMWPE + BS yarns in the front and back side layers (in the cases of 3DS\_VV and 6DS\_HH) have a significant impact on the cut resistance. In the case of 4DS\_HV and 5DS\_VH knitted fabrics, no significant impact on cut resistance has

been identified in changing the arrangement of HMWPE + BS yarns in the front and back side layers.

Based on the cut resistance testing results and assessment of the levels of performance (Table 2), seven out of eight tested knitted fabrics comply with the highest level of the cut resistance, that is, Level F (>30 N).

The cut resistance testing results can be described by a mathematical function (Figure 5):  $CR = -985.3 + 3.82x + 219\ln y$  ( $R^2 = 0.94$ ), where  $CR$  is the cut resistance, N,  $x$  is BS, %, and  $y$  is HMWPE, %.

The cut resistance increases with the decrease in the HMWPE content and increase in the BS content in the knitted structure.

### Puncture resistance

The puncture resistance testing showed that the knitted fabric 1DS composed of 94% HMWPE and 6% PA (Figure 6) required the highest puncture force ( $F_p = 556$  N). The 8DS with the highest BS content (46%) and the lowest HMWPE content (48%) required the lowest puncture force ( $F_p = 302$  N).

Comparison of the puncture resistance testing results of fabrics 1DS and 8DS revealed that the puncture resistance of 1DS is 1.84-fold higher. This difference is due to the different percentage content of raw materials in the structures (Figure 3). The puncture force  $F_p$  tended to decrease with the increase in the BS content and decrease in the HMWPE content in the structure (Figure 6). The testing results of fabric 3DS\_VV showed a substantial decrease in the puncture force  $F_p$ , as more than 20% of BS in the fabric led to a substantial decrease in the puncture force from 556 to 404 N. Meanwhile, further increases in the BS content did not lead to any substantial changes, for example, the puncture force of fabrics 7DS (32% of BS) and 8DS (46% of BS) differed by 3.7% only. Other researchers reporting the lowest puncture force in fabrics with the

**Table 3.** Cut resistance Duncan test result

Knitted fabric	Subset for alpha = 0.05					
	1	2	3	4	5	6
8DS	39.42					
7DS	39.30					
3DS_VV		36.57				
5DS_VH			34.51			
4DS_HV			33.93	33.93		
6DS_HH				33.83		
2DS					31.28	
1DS						7.85

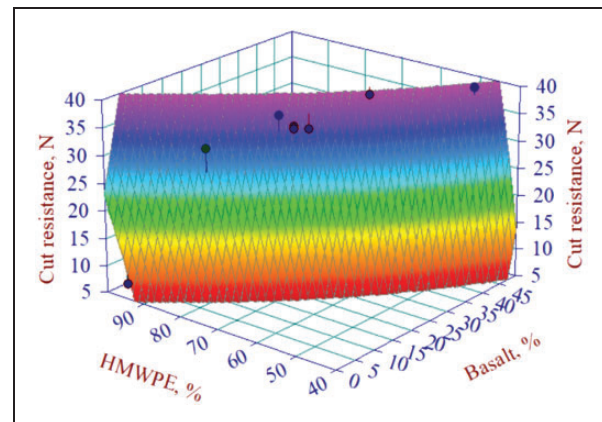


**Figure 5.** The mathematical model for the cut resistance testing results. HMWPE: high molecular weight polyethylene.

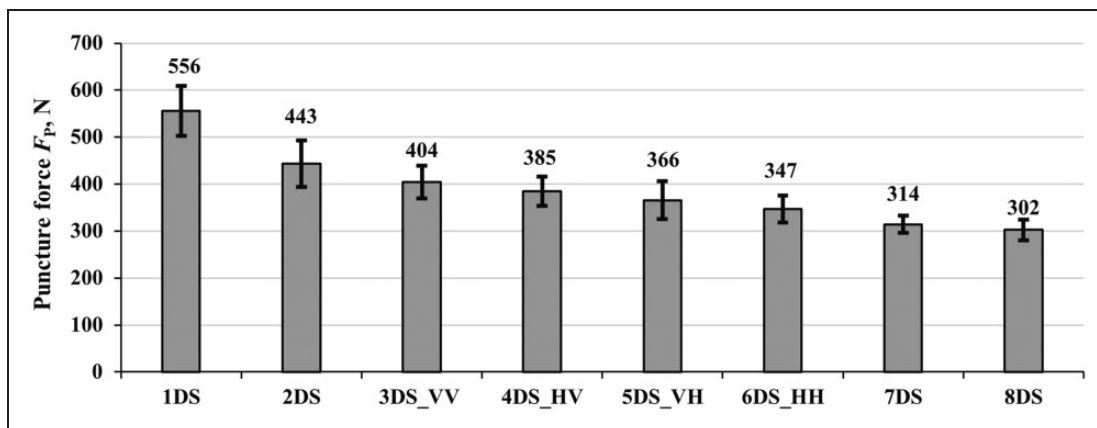


**Figure 6.** Puncture resistance test results (coefficient of variation (CV) = 3.7–7.0%).

highest content of inorganic fibers in the knitted structure, too.<sup>29,39</sup>

Analysis of the puncture resistance testing results in respect of fabrics 3DS\_VV, 4DS\_HV, 5DS\_VH, and 6DS\_HH showed that the knit 3DS\_VV with vertically positioned HMWPE + BS in the front and back side layers was the most puncture-resistant ( $F_p = 404$  N) and the force required to puncture was 14% higher as compared to that required to puncture fabric 6DS\_HH ( $F_p = 347$  N, horizontally positioned HMWPE + BS in the front and back side layers). The results obtained (3DS\_VV, 6DS\_HH) suggest that technical yarn positioning is important for the puncture resistance, except for 3DS\_VV, 4DS\_HV, and 5DS\_VH, for which a significant difference between the puncture resistance values has not been identified (Table 4). After analysis of the testing results of the fabrics with various compositions and structures, fabric 3DS\_VV appears to have the optimal puncture resistance.

The results of the puncture resistance study have been statistically evaluated using the Duncan test (Table 4). It was confirmed that there exists a significant difference between 1DS, 2DS, 3DS\_VV, 6DS\_HH, and 8DS knitted fabrics at the 5% significance level. Thus, not only the changed amount of HMWPE and BS in the structure of the knitted fabric, but also the arrangement of HMWPE + BS yarns in the front and back sides layers (in the cases of 3DS\_VV and 6DS\_HH) have a significant impact on the puncture resistance of the knitted fabrics.

Analysis of the puncture curves of the knits tested (Figure 7(a)) revealed clear differences in the curve-specific inclination angles/Young's modulus. Knit 1DS with the highest HMWPE content produced the largest inclination angle of the curve (Figure 7(b)), which indicates that the knit was difficult to penetrate, the maximum puncture force  $F_p$  was reached, and high

**Table 4.** Puncture resistance Duncan test result

Knitted fabric	Subset for alpha = 0.05					
	1	2	3	4	5	6
1DS	556					
2DS		443				
3DS_VV			404			
4DS_HV			385			
5DS_VH			366	366		
6DS_HH				347	347	
7DS					314	314
8DS						302

resistance encountered. The curve representing knit 8DS with the highest BS content had the lowest inclination angle (Figure 7(b)). The inclination angle of the puncture curve tended to decrease with increasing the BS content. The inclination angles of fabrics 2DS (11% BS) and 3DS (20% BS) were found to be similar at the first stage of puncturing and rather close to the inclination angle of fabric 1DS (94% HMWPE) at the first stage of puncturing.

The puncture curves of the 3D weft-knitted fabrics with different fiber compositions also showed different displacement of the puncture needle. Fabrics with a higher BS content were more extensible, loops were able take more yarn from the adjacent ones, and they extended more in the direction of the needle puncture.

Based on the testing results and assessment of the levels of performance (Table 2), all the knitted fabrics met the highest level of puncture resistance, that is, Level 4.

The puncture resistance testing results can be described by a mathematical function (Figure 8):  $PR = 5648.778 - 21.998x - 1120.341 \ln y$  ( $R^2 = 0.98$ ), where  $PR$  is the puncture force, N,  $x$  is BS, %, and  $y$  is HMWPE, %. The puncture resistance of the structure

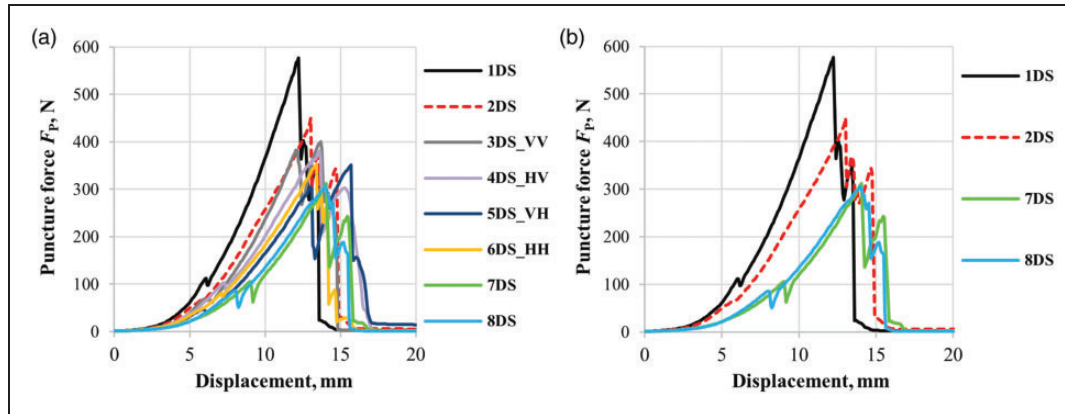


Figure 7. Force–displacement typical curves.

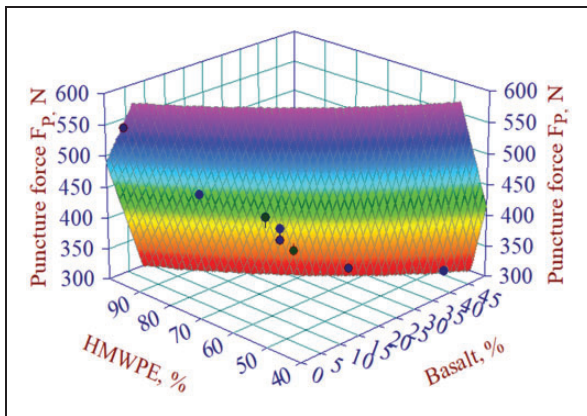


Figure 8. The mathematical model for the puncture resistance testing results. HMWPE: high molecular weight polyethylene.

of the 3D weft-knitted fabric changes with the change in the HMWPE and BS content: the highest puncture resistance was achieved in the knitted structures with the highest HMWPE content, while the increase in the BS content in the knitted structure did not improve the puncture resistance.

### Abrasion resistance

The purpose of the abrasion resistance testing is to determine the number of abrasion cycles required for breakdown involving all layers of the specimen to occur. In two of the eight tested 3D weft-knitted fabrics (1DS, 2DS) no breakdown occurred, so the number of cycles required for the breakdown involving all layers of the fabric to occur was not determined for these fabrics. See Figure 9 for the results of the abrasion testing and Figure 10 for the specimen images after the different number of cycles.

The testing results (Figures 9 and 10) suggest that of all eight tested fabrics, knits 1DS and 2DS, in which no

breakdown occurred even after 20,000 cycles of abrasion, were the most abrasion-resistant. Knits 1DS and 2DS have the highest HMWPE content in their structures as compared to other knits: 1DS contains 94% HMWPE, while 2DS contains 84% HMWPE and 11% BS. The HMWPE content in the structure appeared to provide high abrasion resistance, while the 11% BS content in the structure of 2DS did not have a significant effect on the abrasion resistance, as no breakdown occurred in the fabric 2DS specimens.

The breakdown of 3D weft-knitted fabrics occurred when the HMWPE content in the knitted structure was decreased to 74% and the BS content increased to 20%. Among all knitted fabrics in which breakdown occurred, 3DS\_VV (with vertically positioned HMWPE + BS in the front and back side layers) was the most abrasion-resistant one. Fabric 8DS with the lowest HMWPE content (48%) and the highest BS content (46%) withstood the lowest number of abrasion resistance testing cycles. The abrasion resistance of 8DS was two times lower than that of 3DS\_VV. Given the structural differences of these knitted fabrics, the conclusion can be made that the abrasion resistance decreases with decreasing the HMWPE and increasing the BS content in the knitted structure. A similar trend was observed by other researchers,<sup>29</sup> who investigated the impact of HMWPE and BS on wear resistance and reported a significant decrease in the wear resistance with increasing the BS content in the structure. The testing results demonstrate that the BS content in the knits does not improve the abrasion resistance (based on comparison of knits 1DS and 8DS) and that the abrasion resistance lowers with decreasing the HMWPE content in the knits.

The results of the abrasion resistance study have been statistically evaluated using the Duncan test (Table 5). The results confirmed that there exists a significant difference between 3DS\_VV, 7DS, and 8DS



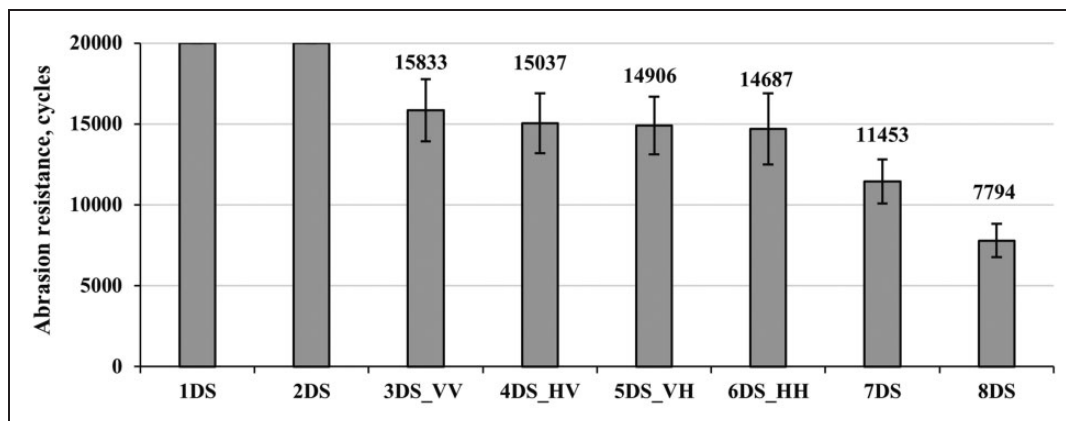


**Figure 9.** Abrasion resistance testing results (CV = 7.5–9.4%).

knitted fabrics at the 5% significance level. Meanwhile, the results of 3DS–6DS materials do not make a significant difference. Thus, the influence of the arrangement of HMWPE + BS yarns in the front and back side layers on the abrasion resistance should be considered insignificant.

Comparison of the specimen images after different numbers of cycles (Figure 10) revealed no significant changes in the appearance of the specimens after 100 and 500 cycles. After 2000 cycles, the front side layer of the knitted fabric 1DS specimens started to break down, while the front side layer of the fabric 8DS specimens was almost completely broken down. Comparison of the specimen images after 8000 cycles revealed that the front side layer of fabric 1DS was not completely broken down; the front side layer of fabric 2DS was completely broken down; the back side layer of fabrics 3DS\_VV, 4DS\_HV, 5DS\_VH, and 6DS\_HH showed the starting signs of breaking down; the back side layer of fabric 7DS was breaking down; meanwhile, the signs of rubbing in the knitted fabric 8DS specimens were recorded before completion of 8000 cycles.

Seven out of eight tested 3D weft-knitted fabrics were able to withstand more than 8000 abrasion cycles and all knitted fabrics meet the highest level, Level 4.

### Tear resistance

Knit 1DS with the highest HMWPE content in the structure showed the highest tearing force as compared to other tested 3D weft-knitted fabrics (Figure 11).

Knit 8DS showed the lowest tearing force (both in the course direction and the wale direction), which was 49–53% lower than that of the 1DS knit. This variation in the results suggests that the tear resistance gradually decreases with decreasing the HMWPE content and

increasing the BS content in the structure of the 3D weft-knitted fabric (Figure 11). Comparison of the 3D weft-knitted fabrics (3DS\_VV, 4DS\_HV, 5DS\_VH, 6DS\_HH) with varied positioning of technical yarns in the front and back side layers showed that a significant effect on tear resistance has been identified only between 3DS\_VV and 6DS\_HH: 6DS\_HH with horizontally positioned HMWPE + BS in the front and back side layers has 27–33% lower tear resistance than 3DS\_VV with vertically positioned HMWPE + BS in the front and back side layers.

The results of the tear resistance study have been evaluated using the Duncan test (Tables 6 and 7). It has been found that there exists a significant difference between tear resistance and the changed amount of HMWPE and BS in the 3D weft-knitted fabric structure at the 5% significant level (in the cases of 1DS, 2DS, 5DS\_VH, 8DS). It has also been found out that there exists a significant difference between the 3DS\_VV and 6DS\_HH knitted fabrics. Therefore, the arrangement of HMWPE + BS yarns in the front and back side layers in the cases of the above-mentioned knitted fabrics also has a significant impact on tear resistance. However, a significant difference between the tear resistance values in changing the arrangement of HMWPE + BS yarns in the front and back side layers has not been identified for the 3DS\_VV, 4DS\_HV, and 5DS\_VH knitted fabrics.

The testing results (Figure 11) show that the tear resistance is 6.5–21.3% higher for the specimens cut in the course direction than for the specimens cut in the wale direction.

All tested 3D weft-knitted fabrics are able to withstand a greater than 75 N load required to tear and meet the highest level, Level 4, according to the EN 388:2016 standard (Table 2). Thus, all the 3D weft-knitted fabrics are suitable for the use in protective wear where high tear resistance is required. In summary

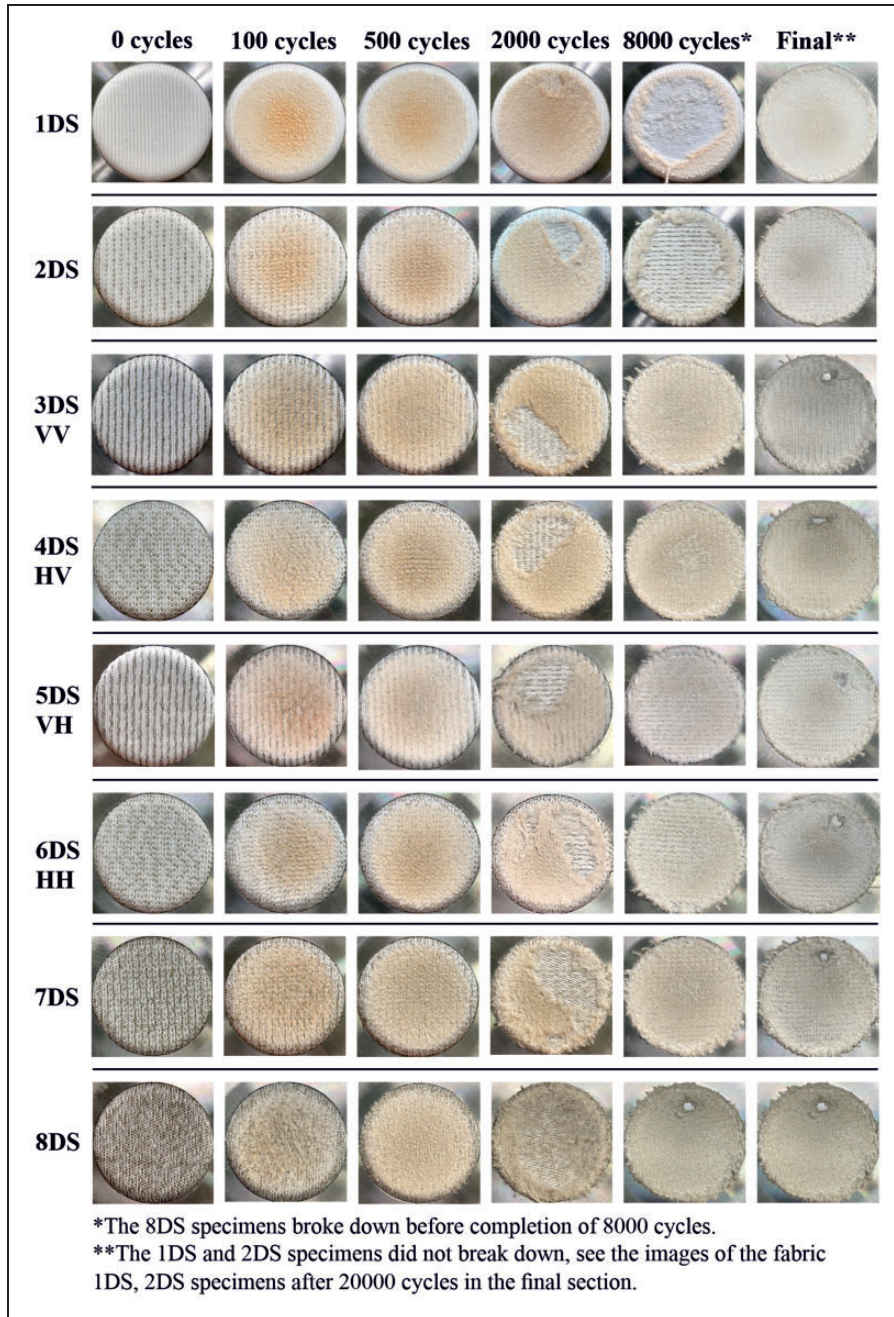


**Figure 10.** Specimen images after different numbers of abrasion cycles.

**Table 5.** Abrasion resistance Duncan test results

Knitted fabric	Subset for alpha = 0.05		
	1	2	3
3DS_VV	15,833		
4DS_HV	15,037		
5DS_VH	14,906		
6DS_HH	14,687		
7DS		11,453	
8DS			7794

of all the fabrics tested, fabric 3DS\_VV (20% BS in the knitted structure) can be mentioned as the optimal variant in terms of the tear resistance, taking into account the impact of both the composition and structure.

The tear resistance testing results can be described by the following mathematical functions:  $F_{TC} = 5916.7 - 27.1x - 1116.5\ln y$  ( $R^2 = 0.87$ );  $F_{TW} = 3826.8 - 17.7x - 692.2\ln y$  ( $R^2 = 0.91$ ), where  $F_{TC}$  is tear resistance (course direction), N,  $F_{TW}$  is tear resistance (wale direction), N,  $x$  is BS, %, and  $y$  is HMWPE, %.

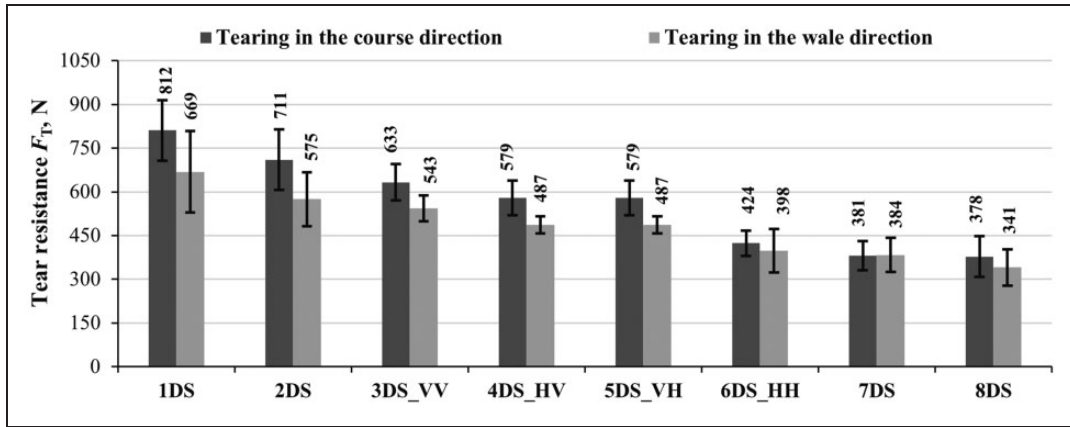


Figure 11. Tear resistance test results (CV = 3.18–12.96%).

Table 6. Tear resistance Duncan test result (tearing in the course direction)

Knitted fabric	Subset for alpha = 0.05			
	1	2	3	4
1DS	812			
2DS		711		
3DS_VV		633	633	
4DS_HV			579	
5DS_VH			579	
6DS_HH				424
7DS				381
8DS				378

Table 7. Tear resistance Duncan test result (tearing in the wale direction)

Knitted fabric	Subset for alpha = 0.05			
	1	2	3	4
1DS	669			
2DS		575		
3DS_VV		543	543	
4DS_HV			487	
5DS_VH			487	
6DS_HH				398
7DS				384
8DS				341

resistance decreases as the HMWPE content decreases and the BS content fabric increases in the knitted structure.

**Conclusions**

Eight 3D weft-knitted fabrics designed for the purposes of this study allowed for investigation of the impact of

the fiber composition on various mechanical risks, while keeping the same stitch density, thickness, and mass per unit area of the 3D weft-knitted fabrics. The cut, puncture, abrasion, and tear resistance testing results suggest the following.

1. The presence of BS in the structure of the 3D weft-knitted fabric has a significant impact on the cut resistance: the use of BS in the knitted structure significantly increases (3.98 (11% BS) to 5-fold (46% BS)) the cut resistance as compared to the knit without BS in the knitted structure.
2. The puncture, abrasion, and tear resistance of 3D weft-knitted fabrics are significantly affected by the HMWPE content in the knitted structure: the highest resistance to these mechanical risks was found in the knitted fabric with no BS in the knitted structure. The decrease in the HMWPE content in the structure of 3D weft-knitted fabrics (from 94% to 46%) reduced the puncture resistance 1.26–1.84 times, abrasion resistance 1.38–2 times, and tear resistance 1.14–2.15 times.
3. The cut, puncture, and tear resistance tests can be described by mathematical functions where  $x$  is the BS content (%) and  $y$  is the HMWPE content (%). The coefficients of determination of the functions  $R^2 = 0.87–0.97$  and can be used to determine the cut, puncture, and tear resistance (N) in the presence of different HMWPE and BS percentage content with 6% PA in the binding layer.
4. When developing knitted fabrics designed to provide protection against mechanical risks, the resistance to different loads can be improved by both varying the percentage content of raw materials and positioning of technical yarns in the structure of 3D weft-knitted fabrics. Testing showed that vertically (VV) positioned HMWPE + BS in the front and back side layers contributed to the achievement of the highest cut, puncture, abrasion, and tear resistance.



5. Vertically (VV) positioned HMWPE + BS in the front and back side layers in the structure of 3D weft-knitted fabrics and 20% BS content in the knitted fabric provided the highest levels of cut, puncture, abrasion, and tear resistance. Therefore, the conclusion can be made that the 3DS\_VV version of the 3D fabric is the optimal one and can be successfully commercialized.
6. Based on the experimental testing results and assessment of the protection levels of 3D weft-knitted fabrics in accordance with the EN 388:2016 standard, the conclusion can be made that the designed fabrics with HMWPE and BS in the knitted structure demonstrate the highest levels of performance: seven out of eight tested 3D weft-knitted fabrics comply with the highest levels of the cut resistance (Level F) and abrasion resistance (Level 4), and all the fabrics comply with the highest levels of puncture and tear resistance. It can be suggested that the 3D weft-knitted fabrics designed provide complex protection against different mechanical risks, such as cut, puncture, abrasion, and tear, and therefore are suitable for use in PPE to reduce the adverse environmental effects on human occupational health.

### Acknowledgment

The authors would like to acknowledge Granberg AS for the support of the investigation.


### Declaration of conflicting interests

The authors have no conflicts of interest to declare.

### Funding

The authors received no financial support for the research, authorship, and/or publication of this article.

### ORCID iD

Julija Krauledaitė  <https://orcid.org/0000-0002-7147-070X>

### References

1. Mollaei A and Ahmadi MS. Effect of structural parameters on the cut resistance of para-aramid and ultra-high molecular weight polyethylene weft knitted fabrics. *J Text Inst* 2020; 111:5; 639–645.
2. Slips, Trips, and Falls: 22 Work Injury Statistics for 2021. <https://legaljobs.io/blog/22-work-injury-statistics/> (2021, accessed 6 November 2021).
3. Ertekin M, Ertekin G and Marmarali A. Analysis of thermal comfort properties of fabrics for protective applications. *J Text Inst* 2018; 109: 1091–1098.
4. Wang L, Yu K, Zhang D, et al. Cut resistant property of weft knitting structure: a review. *J Text Inst* 2018; 109: 1054–1066.
5. Tien DT, Kim JS and Huh Y. Evaluation of anti-stabbing performance of fabric layers woven with various hybrid yarns under different fabric conditions. *Fibers Polym* 2011; 12: 808–815.
6. Li D. *Cut protective textiles*. 1st ed. Sawston: Woodhead Publishing, 2020, p.271.
7. Rebouillat S, Steffenino B and Miret-Casas A. Aramid, steel, and glass: characterization via cut performance testing, of composite knitted fabrics and their constituent yarns, with a review of the art. *J Mater Sci* 2010; 45: 5378–5392.
8. David NV, Gao XL and Zheng JQ. Ballistic resistant body armor: Contemporary and prospective materials and related protection mechanisms. *Appl Mech Rev* 2009; 62: 050802–50822.
9. Tabiei A and Nilakantan G. Ballistic impact of dry woven fabric composites: a review. *Appl Mech Rev* 2008; 61; 010801–10813.
10. Cheeseman BA and Bogetti TA. Ballistic impact into fabric and compliant composite laminates. *Compos Struct* 2003; 61; 161–173.
11. Memon AA, et al. Facile fabrication and comparative exploration of high cut resistant woven and knitted composite fabrics using Kevlar and polyethylene. *Fash Text* 2018; 5: 1–11.
12. LaBarre ED, et al. Effect of a carbon nanotube coating on friction and impact performance of Kevlar. *J Mater Sci* 2015; 50: 5431–5442.
13. Messiry ME, Eloufy A, Latif SA, et al. Evaluation of cutting force of high-performance fibers' dynamic cutting behavior. *J In Text*. Epub ahead of print 28 January 2021. DOI: 10.1177/1528083721990752.
14. Lei J, Dang XA and Li JJ. Characteristic, application and development of basalt fiber. *New Chem Mater* 2007; 35: 9–11.
15. Hrynyk R and Frydrych I. Study on textile assemblies with aluminized basalt fabrics destined for protective gloves. *Int J* 2015; 27: 1–17.
16. Talib AAA, et al. Effect of wear conditions, parameters and sliding motions on tribological characteristics of basalt and glass fibre reinforced epoxy composites. *Materials* 2021; 14: 1–18.
17. Miśkiewicz P, Tokarska M, Frydrych I, et al. Effect of metallisation of basalt fabric on its surface resistivity. *Fibres Text East Eur* 2021; 29: 41–46.
18. Li Z, Ma J, Ma H, et al. Properties and applications of basalt fiber and its composites. *IOP Conf Ser Earth Environ Sci* 2018; 186: 012052.
19. Hao YK and Xiao JY. *High performance composite materials*. Chemical Industry Press, Beijing, 2004, pp.189–192.
20. Hafsa J and Rajesh M. A green material from rock: basalt fiber – a review. *J Text Inst* 2006; 107: 923–937.
21. Gilewicz P, Frydrych I, Cichocka A, et al. Measurement of joint durability between an aluminum foil and basalt fabrics. *Fibres Text East Eur* 2019; 27: 81–84.
22. Hong H and Qing H. Knitting of basalt filament yarn. *Text Res J* 2010; 81: 690–697.
23. Mason K. The still-promised potential of basalt fiber composites. *Composite World*, <https://www.compositesworld.com/articles/the-still-promised-potential-of-basalt-fiber-composites> (2019, accessed 6 November 2021).



24. Frydrych I, Cichocka A, Gilewicz P, et al. Thermal manikin measurements of protective clothing assemblies. *Fibres Text East Eur* 2018; 26: 126–133.
25. Huaian Z, Yiming Y, Deju Z, et al. Tensile mechanical properties of basalt fiber reinforced polymer composite under varying strain rates and temperatures. *Polym Test* 2016; 51: 29–39.
26. Hao LC and Yu WD. Evaluation of thermal protective performance of basalt fiber nonwoven fabrics. *J Therm Anal Calorim* 2010; 100: 551–555.
27. Militky J, Kovacic V and Bajzik V. Mechanical properties of basalt filaments. *Fibres Text East Eur* 2007; 15: 49–53.
28. Fu H, Feng X, Liu J, et al. An investigation on anti-impact and penetration performance of basalt fiber composites with different weave and lay-up modes. *Def Technol* 2020; 16: 787–801.
29. Cao S, Liu H, Ge S, et al. Mechanical and tribological behaviors of UHMWPE composites filled with basalt fibers. *J Reinf Plast Compos* 2011; 30: 347–355.
30. Zineb B and Levent T. A review of recent research on materials used in polymere matrix composites for body armor application. *J Compos Mater* 2018; 52: 3241–3263.
31. Mayo J and Wetzel E. Cut resistance and failure of high-performance single fibers. *Text Res J* 2014; 84: 1233–1246.
32. Alpyildiz T, Icten BM, Karakuzu R, et al. The effect of tuck stitches on the mechanical performance of knitted fabric reinforced composites. *Compos Struct* 2009; 89: 391–398.
33. EN ISO 139:2005. Textiles — standard atmospheres for conditioning and testing.
34. EN ISO 5084:1996. Textiles – determination of thickness of textiles and textile products.
35. LST EN 12127:1999. Textiles – fabrics – determination of mass per unit area using small samples.
36. EN ISO 13997:1999. Protective clothing — mechanical properties — determination of resistance to cutting by sharp objects.
37. EN 388:2016+A1:2018. Protective gloves against mechanical risks.
38. Irzmanska E and Stefka A. Comparative evaluation of test methods for cut resistance of protective gloves according to Polish standards. *Fibres Text East Eur* 2012; 20: 99–103.
39. Ertekin M and Kirtay HE. Cut resistance of hybrid para-aramid fabrics for protective gloves. *J Text Inst* 2016; 107: 1276–1283.